

N65-32082

FACILITY FORM 802

(ACCESSION NUMBER)
61
(PAGES)
CR 64432
(NASA CR OR TMX OR AD NUMBER)

(THRU)
1
(CODE)
30
(CATEGORY)

GPO PRICE \$ _____

CFSTI PRICE(S) \$ _____

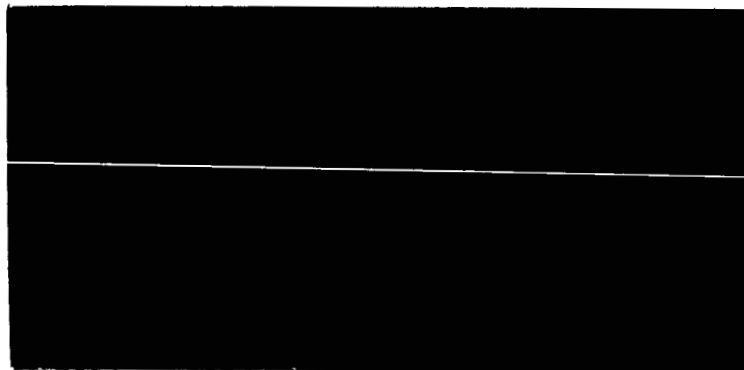
Hard copy (HC) 3.00

Microfiche (MF) .75

ff 653 July 65



Bedford, Massachusetts



National Aeronautics and Space Administration
Headquarters
Washington, D.C.

20 July 1965

GCA CORPORATION
GCA TECHNOLOGY DIVISION
Bedford, Massachusetts

PLANETARY METEOROLOGY
Quarterly Progress Report No. 1
Covering the Period
21 March 1965 - 30 June 1965

Contract No. NASW-1227

SUMMARY

During the first three months of the current contract, emphasis has been placed on the meteorology of Mars, although some research has also been performed on the meteorology of Venus. The following studies are under way:

Seasonal Climatology of Mars — In this study, simple theoretical models are developed for determining the seasonal and latitudinal variations of surface temperature and mean atmospheric temperature. In one model, the surface and mean atmospheric temperatures are computed from conditions of radiative equilibrium. In a second model, the effect of the meridional transport of heat by the atmosphere is included in the computations of the Martian temperature climate.

Diurnal Variation of the Surface Temperature on Mars — A theoretical model of the diurnal variation of surface temperature is developed. In the model, the planetary surface receives and loses energy by the following processes: absorption of solar radiation, emission of long-wave radiation, absorption of atmospheric long-wave radiation, eddy conduction of heat between the surface and atmosphere, and molecular conduction of heat between the surface and soil layer. This model should be more realistic than the one used by Sinton and Strong (1960) to explain the observed indications of the diurnal temperature variation at the Martian surface.

Interhemispheric Transport of Water Vapor and the Martian Ice Caps -

Since the observed amount of water vapor in the Martian atmosphere is much less than that required to form the Martian ice caps, it has been suggested that the source of the water vapor for the forming ice cap is the water vapor released into the atmosphere by the melting cap. Studies have been begun to determine whether large-scale eddy diffusion processes, with reasonable values of eddy diffusion coefficients, can indeed accomplish the necessary shuttling of water vapor from pole to pole within the required time periods.

A Comparison of Zonal Wind Velocities on Mars and Earth - Based upon Gifford's (1964) data on projection cloud motions, average zonal velocities as a function of Martian latitude are derived. These values are compared with average zonal velocities for the Earth's troposphere. The general shapes of the curves representing the latitudinal variation of zonal velocity are similar, both being characterized by maximum westerlies at middle latitudes. More detailed conclusions are not warranted at this time since the Martian data sample is extremely small and the interpretation of Martian cloud drifts as wind velocities - rather than storm velocities - is open to question.

Atmospheric Circulation in the Venusian Atmosphere - Attempts to solve by finite difference techniques the equations resulting from the convective model of the general circulation of the Venusian atmosphere described in our Final Report on NASw-975 have been unsuccessful. A new approach to the solution of the equations is being investigated.

Rather than using finite difference techniques, Fourier series solutions are assumed for the dependent variables. By linear algebraic techniques, it should be possible to determine the coefficients of the assumed Fourier series.

The Composition of the Venusian Clouds - One of the arguments that have been presented against a water or ice composition for the Venusian clouds is based upon a comparison of the water vapor mixing ratio in the Venusian atmosphere, as deduced from spectrometric observations of atmospheric water vapor abundance, with the mixing ratio required for water vapor saturation at the temperature and pressure of the Venusian cloud-top. Such a comparison indicates that the observed mixing ratio is far below that required for saturation. However, the deduction of the water vapor mixing ratio has been based upon the assumption that the mixing ratio is constant with altitude. In the Earth's atmosphere, the water vapor mixing ratio decreases rapidly with height, especially in the upper troposphere. In this study, we compute the water vapor mixing ratio that would be present at the level of the Venusian cloud-top if, on Venus, the mixing ratio decreases with altitude at rates comparable to those in the Earth's atmosphere. The total water vapor amount is kept compatible with the observed amounts. Comparison of the cloud-top mixing ratio computed in this manner with the required saturation mixing ratio reveals that, under certain conditions, saturation can indeed be achieved. Thus, under certain conditions, the observed water vapor amounts are not incompatible with a Venusian cloud composed of ice.

TABLE OF CONTENTS

<u>Section</u>	<u>Title</u>	<u>Page</u>
	SUMMARY	i
1	METEOROLOGY OF MARS	1
	1.1 The Seasonal Climatology of Mars	1
	1.2 Diurnal Variation of the Surface Temperature of Mars	18
	1.3 Interhemispheric Transport of Water Vapor and the Martian Ice Caps	32
	1.4 A Comparison of Zonal Wind Velocities on Mars and Earth	39
2	METEOROLOGY OF VENUS	42
	2.1 Atmospheric Circulation in the Venusian Atmosphere	42
	2.2 The Composition of the Venusian Clouds	48
	REFERENCES	55

SECTION 1

METEOROLOGY OF MARS

1.1 THE SEASONAL CLIMATOLOGY OF MARS

1.1.1 Introduction. The climate on Mars has been a subject of debate since the invention of the telescope. The basis for a study of Martian climatology is the welding together of available observational data and appropriate theory. Prior to the early radiometric measurements of Mars by Coblentz and Lampland (1923), estimates of Martian climatology used visual and photographic observations in order to calculate surface and atmospheric temperatures, e.g., Milankovitch (1920). Gifford (1956) has summarized radiometric measurements of Mars over the years in a seasonal climatology of the surface-temperature distribution. Recently measurements by Sinton and Strong (1960), and by Kaplan, Munch and Spinrad (1964), have increased our knowledge about the diurnal temperature variation and composition of the Martian surface, and about the total pressure and composition of the atmosphere of Mars, respectively. In light of these recent measurements, a study of the seasonal variations of the Martian climate seems appropriate at this time.

Recent research emphasis has centered around investigations of the temperature structure of the Martian atmosphere, e.g., Goody (1957),

Arking (1963), Ohring (1963), and Prabhakara and Hogan (1965). The results of these investigations are based on calculations using multi-layered model atmospheres which generally apply to the average Martian latitude and climate. In a climatological study, however, the need for a detailed vertical temperature structure with latitude and time of year is secondary to the inferred climatic variations. Instead of using a sophisticated multilayered model atmosphere, this study incorporates a single-layered atmosphere in order to reduce the computing time and to emphasize the changes in climate. The loss in accuracy when using the single-layered model is no greater than the error introduced by the uncertainty in total pressure and composition of the Martian atmosphere.

The remaining discussion in this section of the report describes the theoretical basis for two model atmospheres to be used in the study of Martian climatology. One model, termed the "Radiative Equilibrium Model," is used to compute the temperature of the surface and the mean temperature of the atmosphere under conditions of radiative equilibrium. In this model, the atmosphere is assumed stationary; i.e., there is no transport of heat. Calculations based on the Radiative Equilibrium Model will describe the extreme or upper limit of the seasonal variations on Mars.

The second model atmosphere, termed the "Radiative Model with Transport of Heat," includes the meridional transport of heat in the calculation of surface and atmospheric temperatures. As is the case on Earth, the transport of heat on Mars tends to moderate seasonal climates. The

polar latitudes will be warmer and the equatorial latitudes will be cooler than the climatic temperatures described by the Radiative Equilibrium Model. A by-product of the calculations using this model will be the variation of the meridional component of the mean atmospheric wind with latitude.

1.1.2 Radiative Equilibrium Model. In any planetary heat budget study, the fundamental law of energy conservation is a basic assumption. This law states that the sources of energy, principally solar or short-wave radiation absorbed by the surface and atmosphere, are balanced by the losses of energy, the emission of radiation to space.

The radiative equilibrium temperatures of the surface and atmosphere depend on the magnitude of the incoming solar energy and on the absorbing and emitting properties of the surface and atmosphere. The interplay of energy between the sun, Mars and space can be described by two energy balance equations, one for the surface and the other for the atmosphere. First, let us examine the important radiation components of a unit atmospheric column shown in Figure 1 and then develop the balance equations from these components.

Of the short-wave radiation incident at the top of the atmosphere ①, a small portion is absorbed by the atmosphere ② before reaching the surface. A major portion of the solar radiation is absorbed by the surface ③ and the remaining energy is diffusely reflected back to the atmosphere ④ and to space ⑤. In the model, atmospheric scattering

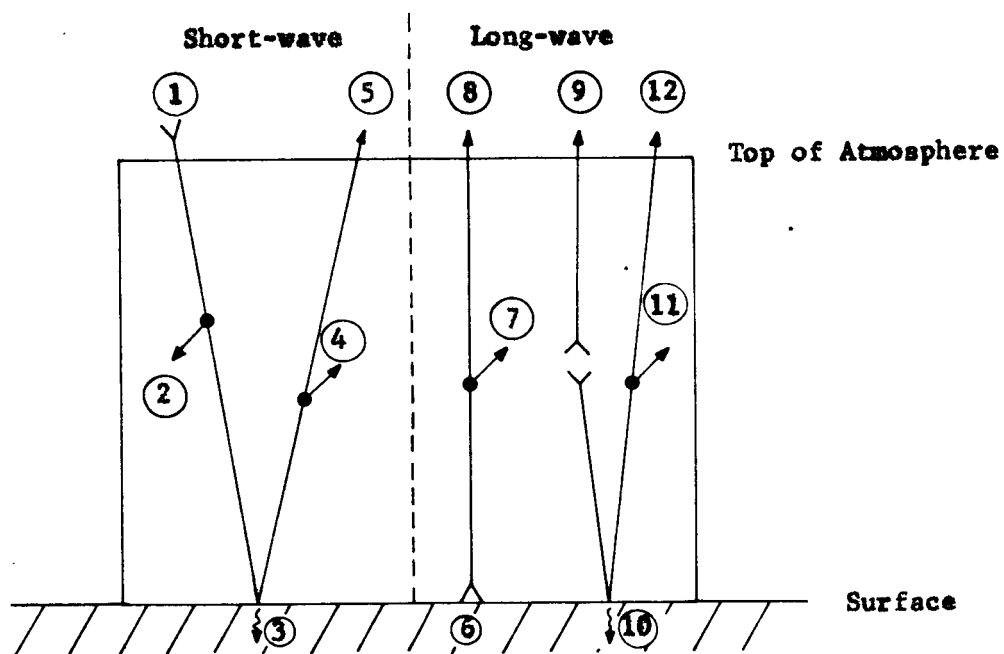


Figure 1. Radiation components of a unit atmospheric column.

of energy is neglected and the atmosphere is assumed free of clouds. The planetary albedo of Mars is controlled mostly by the assumed surface reflectivity and to a lesser degree by atmospheric absorption.

In turn the surface emits long-wave radiation (6) back to the atmosphere (7) and to space (8). The atmosphere emits radiation to space directly (9) and emits radiation back to the surface. A major portion of this back radiation from the atmosphere is absorbed at the surface (10) ; a small portion is reflected back to the atmosphere (11) and to space (12) .

In the Radiative Equilibrium Model, the gains and losses of energy at the top of the atmosphere, within the atmosphere and at the surface must all be equal; i.e., the net radiation is zero. The exchange of sensible heat at the surface-atmosphere interface is neglected in this model. The energy balance equation for the surface is

$$(1 - R_{s_o}) F_{s_o} + \epsilon_o \epsilon_a \sigma T_a^4 = \epsilon_o \sigma T_o^4, \quad (1)$$

where R_{s_o} = the surface reflectivity to short-wave radiation
 F_{s_o} = the incident short-wave radiation at the surface
 ϵ_o = the surface emissivity to long-wave radiation
 ϵ_a = the atmospheric emissivity to long-wave radiation
 σ = Stefan- Boltzmann's constant
 T_a = the mean atmospheric temperature in $^{\circ}\text{K}$
 T_o = the surface temperature in $^{\circ}\text{K}$.

The gains of energy to the left of Equation (1), respectively, are the absorbed short-wave radiation and the absorbed long-wave radiation emitted by the atmosphere. Both terms are balanced by the surface radiant energy loss.

The energy balance equation for the atmosphere is

$$[F_{s_t} - F_{s_o} (1 - R_{s_o}) (1 - e^{-1.66\tau})] + \epsilon_a \epsilon_o \sigma T_o^4$$

$$= [2 - (1 - \epsilon_o) \epsilon_a] \epsilon_a \sigma T_a^4, \quad (2)$$

where F_{s_t} = the insolation at the top of the atmosphere

τ = the optical thickness of the atmosphere to short-wave radiation

$e^{-\tau}$ = the vertical beam transmissivity of the atmosphere to direct short-wave radiation

$e^{-1.66\tau}$ = the transmissivity of the atmosphere to diffuse short-wave radiation.

The first term in brackets to the left of Equation (2) is the solar energy absorbed by the atmosphere, both the direct component and diffusely reflected component from the surface, and the second term is the absorbed long-wave radiation from the surface. These energy gains are balanced by the radiant energy loss to the surface and space. The $(1 - \epsilon_o) \epsilon_a$ correction term accounts for the small portion of back long-wave radiation that is reflected by the surface and absorbed again by the atmosphere.

In the model atmosphere, Kirchoff's law is assumed to hold for a given spectral region; e.g., the emissivity equals the absorptivity for long-wave radiation.

There are two energy balance equations, (1) and (2), with two dependent variables, T_a and T_o ; therefore, a solution for the equilibrium surface and atmospheric temperatures is possible. After an exercise in algebra, the solution for the surface temperature is

$$T_o = \left\{ \frac{(1 - R_{s_o}) F_{s_o} + \epsilon_o [F_{s_t} - F_{s_o} (1 - R_{s_o}) (1 - e^{-1.66\tau})]}{\epsilon_o \sigma} \right\}^{1/4}, \quad (3)$$

and the solution for the atmospheric temperature is

$$T_a = \left\{ \frac{\epsilon_a (1 - R_{s_o}) F_{s_o} + F_{s_t} - F_{s_o} (1 - R_{s_o}) (1 - e^{-1.66\tau})}{\epsilon_a (2 - \epsilon_a) \sigma} \right\}^{1/4}. \quad (4)$$

The all-important energy source on which the study of theoretical climatology rests is the amount of solar radiation received by the planet. This can be computed with the aid of an assumed solar constant and a knowledge of astronomical geometry. The daily energy incident on a unit surface at the top of the atmosphere is

$$F_{s_t} = \frac{S[(\sin \theta \sin \delta) \beta + \cos \theta \cos \delta \sin \beta]}{\pi d^2} \quad (5)$$

where $\cos \beta = -\tan \theta \tan \delta$

θ = the latitude of the unit area

δ = the solar declination

β = the hour angle between sunrise and noon or noon and sunset

S = the solar constant for the Earth

d = the distance of Mars from the sun in astronomical units.

A second component of solar radiation that is important in this study is the insolation at the surface, F_{s_0} . An analytic solution of this component is not possible as in the case of Equation (5) above since the absorption of solar radiation by the atmosphere at each sun angle must be summed over all angles during the daylight hours. The equation for the insolation incident on a unit surface area over an increment time span, dt , is

$$\frac{d F_{s_0}}{dt} = \frac{S(e^{-\tau})^m \cos \phi}{d^2}, \quad (6)$$

where ϕ = the sun's zenith angle

m = the optical air mass.

Equation (6) is assumed to hold for all wavelengths of solar radiation although, strictly speaking, it applies only to monochromatic radiation. As Fritz (1951) points out, the use of Beer's law in Equation (6) for a given spectral region will lead to practical results. Numerical integration of Equation (6) gives the solar insolation at the surface to a reasonable degree of accuracy.

Summarizing the Radiative Equilibrium Model, the atmosphere of Mars is depicted as a single isothermal layer with gray spectral properties in the long-wave and short-wave regions of the spectrum. Atmospheric scattering is neglected; however, it is intrinsically implied in the surface albedo term. Also the surface albedo determines to a great extent the planetary albedo. The computed equilibrium temperatures of the surface and atmosphere are based on the incoming solar radiation and on the absorbing and emitting properties of the surface and atmosphere.

A more sophisticated depiction of the atmosphere could be derived using a multilayered model and the method outlined above. However, it is felt that the uncertainties in the input parameters to the model outweigh the bias introduced by the single-layer model.

Since the atmosphere is assumed stationary, the computed mean daily temperatures will represent the extreme climatic conditions on Mars. Atmospheric circulations transport heat from warm latitudes to cold latitudes, thus moderating the climate. A model atmosphere which includes this atmospheric transport of heat is discussed in the next section.

1.1.3 Radiative Model with Transport of Heat. In the discussion of atmospheric heat transport on Mars, let us picture the atmosphere as being divided into 10° latitude zones as shown in Figure 2, and that the radiation budget at the midpoint of each zone applies to the whole zone.

As mentioned in the previous section, the equilibrium temperatures of the atmosphere depend primarily on the amount of incoming solar

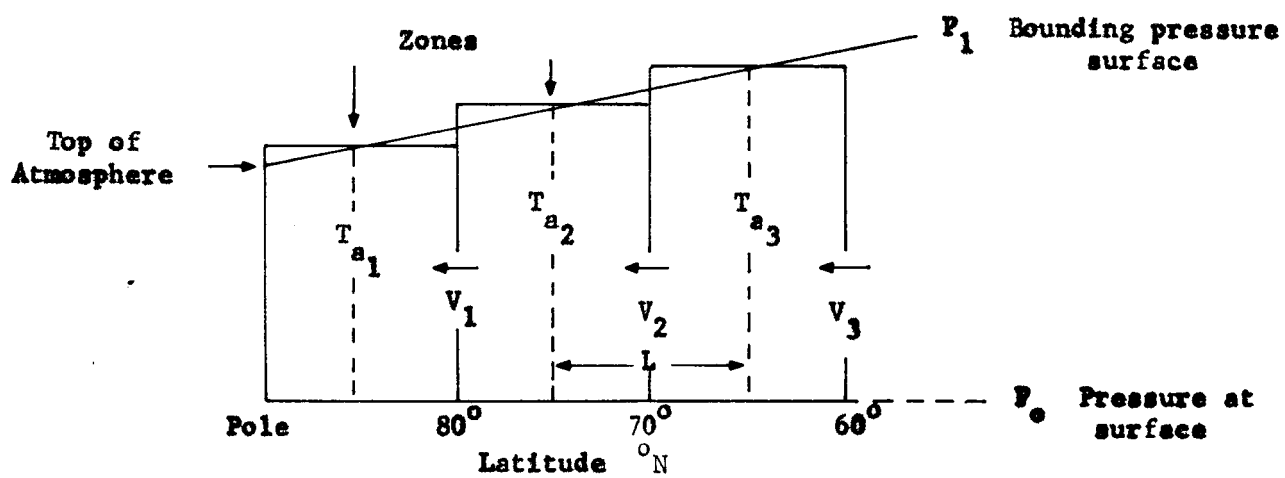


Figure 2. Division of atmosphere into columns.

radiation. Take, for example, the Martian vernal equinox where the sun is positioned over the equator. Under these conditions the equator receives the maximum amount of solar radiation with a steady decrease of input toward both polar latitudes. Based on calculations using Equation (4), the atmospheric temperatures decrease steadily poleward of the equator. Consequently, a north-south temperature gradient is established, and an atmospheric transport of heat would commence from equator to poles, sustained by the differential solar heating.

Our objective in this model atmosphere is to determine the equilibrium temperatures of the surface and atmosphere with the transport of heat included in the calculations. It should be emphasized again that the law of energy conservation is assumed, and that the total gain of energy by all the atmosphere on Mars is the same, with or without heat transport. Likewise, the total loss of energy by the atmosphere is the same, even though colder latitudes will be warmed by heat transport. This fact serves as a boundary condition to the problem.

Haurwitz (1961) has studied simple models of atmospheric circulation that can be adapted to this problem. In his model he assumes that the temperature difference in the horizontal between two pressure surfaces is established and maintained by some outside agency, such as differential solar heating. He shows that the resulting atmospheric motion that is established and maintained by differential heating approaches definite values of velocity and corresponding temperature difference. The magnitudes of velocity and temperature difference depend on the Coriolis

parameter due to the planet's rotation, on the assumed coefficient of friction, on the rate of heating, on the dimensions of the model and not on the initial conditions.

Rather than writing Haurwitz's equations in terms of heating rates (degrees/unit of time), it is more convenient to write the differential heating term in units of a radiant flux density. The modified form of his equation for the equilibrium wind velocity is

$$V_n = \frac{1}{2} \left[\frac{\alpha_n g R^* \ln \frac{P_o}{P_1}}{P_o C_p \left(1 + \frac{f_n^2}{k^2} \right)} \right]^{1/2} \quad (7)$$

and for the equilibrium temperature difference is

$$T_{a_{n+1}} - T_{a_n} = \left[\frac{\alpha_n g L^2 K \left(1 + \frac{f_n^2}{k^2} \right)}{C_p P_o R^* \ln \frac{P_o}{P_1}} \right]^{1/2} \quad (8)$$

where n = the boundary between the n and $n+1$ zones of Figure 2. The zones are numbered consecutively starting at $85^\circ N$ in increments of 10° latitude (18 zones in all)

V_n = the wind velocity between adjacent zones in Figure 2 (17 velocities in all)

α_n = the differential heating in units of $\text{cal cm}^{-2} \text{min}^{-1}$ between the n and $n+1$ zones

g = the gravity on Mars

R^* = the specific gas constant for the Martian atmosphere

- P_0 = the pressure at the surface of Mars
- P_1 = the bounding pressure surface at the "top of the atmosphere" in Figure 2
- C_p = the specific heat capacity of the atmosphere at constant pressure
- K = the coefficient of friction
- f_n = the Coriolis parameter between the n and $n+1$ zones
- L = the horizontal dimension of the model taken to be the distance between zones in Figure 2, 10° of latitude

The differential heating between zones, α , is the sustaining source of energy that drives the circulation. In other words, it is the heat flux transported across the imaginary wall between zones that must be dissipated in the cooler zone or transported to the next colder zone.

Since the goals of the calculations are the equilibrium temperatures of the atmosphere and surface, it is more convenient to use Equation (8) which relates temperature differences to differential heat fluxes between zones rather than the wind velocity in Equation (7). A correction for zonal areas is also necessary in Equation (8) for the following reason: Take, for example, the wind velocity V_1 in Figure 2, which indicates that heat is transported from zone 2 to zone 1. The area of zone 2 is larger than zone 1; therefore, the radiant flux density of heat transported to zone 1, α_1 , must be increased by the ratio of areas of the zone, i.e., the area of zone 2 divided by the area of zone 1. Conversely, if V_1 were a south wind, α_1 would be reduced by the ratio of areas, the area of zone 1 divided by the area of zone 2. The direction of wind, sign

of α_n and sense of the area ratio correction is determined by the relative magnitudes of solar heating since heat flows from the zone of greater heating to the zone of lesser heating.

To simplify the algebra in this development, let us write Equation (8) as

$$C_n (T_{a_{n+1}} - T_{a_n})^2 = \alpha_n \quad (9)$$

where C_n is a lumped term of known values including the correction for zonal areas A_n ,

$$C_n = \frac{A_n C_p P_o R^* \ln \frac{P_o}{P_1}}{g L^2 K \left(1 + \frac{f_n^2}{k^2} \right)}$$

Again the equilibrium temperature achieved by a zone is calculated from the energy gains and losses. The net radiation of a zone equals the export of heat out of a zone. The difference between the absorbed solar radiation for a zone, call it S_n equal to $\epsilon_a (1 - R_{s_o}) F_{s_o} + F_{s_t} - F_{s_o} (1 - R_{s_o}) (1 - e^{-1.66\tau})$ from Equation (4) and the emitted long-wave radiation, $e T_{a_n}^4$, where $e = \epsilon_a (2 - \epsilon_a)$, must equal the net export of heat out of the zone ($\alpha_{n-1} - \alpha_n$). Thus, a set of eighteen equations can be written for the energy balance of each zone.

$$\begin{aligned}
s_1 - e T_{a_1}^4 &= -\alpha_1 \\
s_2 - e T_{a_2}^4 &= (\alpha_1 - \alpha_2) \\
s_3 - e T_{a_3}^4 &= (\alpha_2 - \alpha_3) \\
&\vdots \\
s_{17} - e T_{a_{17}}^4 &= (\alpha_{16} - \alpha_{17}) \\
s_{18} - e T_{a_{18}}^4 &= \alpha_{17}
\end{aligned} \tag{10}$$

Based on the sign convention, a positive value of α_n represents a north wind in Equation (7); a negative value of α_n represents a south wind.

After substitution of Equation (9) in Equation set (10), the energy balance of each zone is expressed only in terms of atmospheric temperatures.

$$\begin{aligned}
s_1 - e T_{a_1}^4 &= -C_1 (T_{a_2} - T_{a_1})^2 \\
s_2 - e T_{a_2}^4 &= C_1 (T_{a_2} - T_{a_1})^2 - C_2 (T_{a_3} - T_{a_2})^2 \\
&\vdots \\
s_{17} - e T_{a_{17}}^4 &= C_{16} (T_{a_{17}} - T_{a_{16}})^2 - C_{17} (T_{a_{18}} - T_{a_{17}})^2 \\
s_{18} - e T_{a_{18}}^4 &= C_{17} (T_{a_{18}} - T_{a_{17}})^2
\end{aligned} \tag{11}$$

Equation set (11) prescribes the equilibrium temperatures of the atmosphere for each zone. Given a value for the first temperature, T_{a_1} , the value of T_{a_2} is computed using the first equation. Using the value of T_{a_2} in the second equation, T_{a_3} is computed using the second equation, etc. This cascade of temperature calculations continues until the eighteenth equation is encountered. The last equation is used as a test to determine whether the proper initial temperature was correctly chosen.

The above calculation procedure is iterated on a computer, using different values of T_{a_1} , until the solution of atmospheric temperatures for Equation (11) is determined.

Summarizing the Radiative Model with Transport of Heat, the Radiative Equilibrium Model of the last section is expanded to include the meridional transport of heat. The transport calculation is based on the simple circulation model developed by Haurwitz and adapted to the specific problem in this model atmosphere. Once the temperatures are known for each zone, the computed values of α_n in Equation (9) can be substituted into Equation (7) to determine the mean meridional wind component for every 10° of latitude. Also the equilibrium surface temperature can be computed once the atmospheric temperatures are known using Equation (3). The entire calculation of winds and temperatures for all latitudes can be carried out for any time of the Martian year.

1.1.4 Status of Work and Future Plans. The status of work on the study of the seasonal climatology of Mars is as follows:

(1) A computer program to calculate the insolation at the top of the atmosphere using Equation (5) for any latitude and time of year is written and checked out.

(2) A computer program to calculate the insolation at the surface by numerical integration of Equation (6) for any latitude and time of year is written and checked out.

(3) A computer program to calculate the radiative equilibrium temperatures of the surface and atmosphere, using Equations (3) and (4), is written and checked out.

Future plans during the next three-month period include:

(1) The modification of the program in paragraph (3) above to include heat transport as discussed in the previous section and specified by Equation set (11).

(2) A search of the literature for the latest information about measured parameters on Mars for input into the model atmosphere.

(3) The calculation of the seasonal climatology of Mars based on both models and evaluation of the results.

(4) The exploration of possible improvements in the model atmospheres. For example, changing the surface albedo after formation of the polar ice cap, including the sensible heat transfer at the surface-atmosphere interface, and including heat conduction into the surface layers and heat storage in the surface and atmosphere.

1.2 DIURNAL VARIATION OF THE SURFACE TEMPERATURE OF MARS

1.2.1 Introduction. For the design of spacecraft to land on the planet Mars, knowledge of meteorological parameters in the Martian planetary boundary layer is required. Pressure, wind, and temperature are of prime interest. In this section, the diurnal variation of the surface temperature of Mars is considered.

Sinton and Strong (1960) obtained observational indications of the diurnal variation of Martian surface temperature. In a theoretical model, they attempted to reproduce the observed diurnal variation. They considered the planetary surface to be heated by solar radiation, and cooled by emission of long-wave radiation and conduction into the soil. The theoretical results were somewhat different from the observational results. The major reason for the discrepancy may be the neglect of the effect of the Martian atmosphere on the surface temperature. This effect is twofold - a heating of the surface due to downward long-wave radiation by the atmosphere and an exchange of heat between surface and atmosphere by eddy conduction. The purpose of this study is to develop and utilize an improved theoretical model - one that includes the effect of the atmosphere - for determining the diurnal variation of Martian surface temperature.

1.2.2 Differential Equation. Our model consists of two semi-infinite layers - the atmospheric layer and the soil layer - on either side of the planetary surface. In the atmospheric layer we assume that there is no mean motion and that, because of the small amount of water vapor and carbon dioxide, radiational heat exchange is negligible compared to eddy conduction of heat. Thus the fundamental equation for the

atmospheric temperature is the equation of eddy conduction of heat,

$$\frac{\partial \theta}{\partial t} = \frac{\partial}{\partial z} \left(\kappa \frac{\partial \theta}{\partial z} \right), \quad 0 \leq z \leq \infty, \quad (12)$$

where θ = potential temperature

$\kappa = \frac{k}{\rho c}$ = exchange coefficient of heat

k = coefficient of diffusivity

ρ = atmospheric density

c = specific heat at constant pressure

z = vertical coordinates with origin at solid surface and positive in the upward direction

t = time .

There have been many expressions for k by various workers. In general, it is a function of height, wind shear and thermal stability (Lettau, 1951; Estoque, 1962; and Wu, 1965). Since we are primarily interested in the surface temperature, the form of the exchange coefficient of diffusivity, k , can be chosen as

$$k = \bar{K} (z + z_0) \quad (13)$$

where \bar{K} is a constant (Lettau, 1951). This expression has also been used by Haurwitz (1936) in the study of the daily temperature period in the lower layer of the Earth's atmosphere. Their results agree reasonably well with the observed data. Now after substituting Equation (13) into Equation (12), we obtain

$$\frac{\partial \theta}{\partial t} = \frac{k'}{\rho c} (1 + \alpha z) \frac{\partial^2 \theta}{\partial z^2} + \frac{k'_0 \alpha}{\rho c} \frac{\partial \theta}{\partial z} \quad 0 \leq z \leq \infty \quad (14)$$

where $k' = \frac{\bar{K}}{z_0}$, and $\alpha = \frac{1}{z_0}$.

For the soil layer, the differential equation of heat conduction is similar to Equation (12) except that the diffusivity of the soil, κ_s , is different from that of the atmosphere. The differential equation of the conduction of heat in the soil can be written as

$$\frac{\partial T_s}{\partial t} = \kappa_s \frac{\partial^2 T_s}{\partial z^2} \quad -\infty \leq z \leq 0, \quad (15)$$

where T_s = temperature of the soil

$\kappa_s = \frac{\bar{K}_s}{\rho_s c_s}$ = diffusivity of the soil

\bar{K}_s = thermal conductivity of the soil

ρ_s = density of the soil

c_s = specific heat of the soil.

If the solutions for Equations (14) and (15) can be solved for suitable boundary conditions, then the surface temperature can be obtained. The boundary condition will be discussed in the next section.

1.2.3 Boundary Conditions. The magnitude of the temperature must be finite both in the soil and the atmosphere at a large distance from the surface. The quantity, z , is taken as zero at the interface of the atmosphere and the soil and increases with height. It is assumed that

$$T_s, \theta < \infty \quad \text{at } z = \pm \infty \quad (16)$$

The remaining two boundary conditions will be deduced at the interface, $z=0$. It is natural to assume that the temperatures are continuous at this interface, i.e.,

$$T_s = \theta \quad \text{at } z = 0 . \quad (17)$$

Since we want to study the diurnal march of the surface temperature, the source of the energy input is the direct insolation from the sun. Because of conservation of energy, there must be an energy balance at an infinitesimally thin layer at the surface $z = 0$. Thus, the algebraic sum of the energy flux must be zero. Then,

$$R + R_a + F_a + F_s + S = 0 \quad (18)$$

where R = long-wave radiation from the surface

R_a = back long-wave radiation from the atmosphere to surface

F_a = the flux of energy at the surface due to eddy heat conduction between surface and atmosphere

F_s = the flux of energy at the surface due to molecular heat conduction between surface and soil

S = insolation at the surface .

If we assume that the conductive flux is in the direction of $+z$, then the upward flux can be written as

$$-k \frac{\partial \theta}{\partial z} \quad \text{or} \quad -\bar{K}_s \frac{\partial T_s}{\partial z} ,$$

and the downward heat flux, in the negative direction of z , is

$$+k \frac{\partial \theta}{\partial z} \quad \text{or} \quad \bar{K}_s \frac{\partial T_s}{\partial z}$$

If, in Equation (18) a downward flow of energy at the surface is considered negative and upward flow at the surface positive, the different terms in the equation of energy at the interface can be written as

$$R = \sigma T_s^4$$

$$R_a = -\alpha \sigma T_s^4$$

$$F_a = -k \left. \frac{\partial \theta}{\partial z} \right|_{z=0}$$

$$F_s = +\bar{K} \left. \frac{\partial T_s}{\partial z} \right|_{z=0}$$

$$S = -\mu I_\infty (\sin \phi \sin \delta + \cos \phi \cos \delta \cos \psi)$$

where σ = Stefan-Boltzmann constant
 α = fraction
 μ = one minus the planetary albedo
 I_∞ = the solar constant
 ϕ = latitude
 δ = solar declination
 ψ = solar hour angle .

In the expression for the back radiation from the atmosphere, R_a , it has been assumed that this quantity is some fraction, α , of the long-wave radiation from the surface. Recent computations (Ohring and Mariano, 1965) suggest that α is about 0.15.

Finally, the energy equation can be written as

$$(1 - \alpha) \sigma T_s^4 - k \left. \frac{\partial \theta}{\partial z} \right|_{z=0} + \bar{K} \left. \frac{\partial T_s}{\partial z} \right|_{z=0} - \int_0^{\mu I_\infty (\sin \phi \sin \delta + \cos \phi \cos \delta \cos \psi)} = 0 \quad (19)$$

in which the upper part of the last term is for the daytime and the lower part, for the nighttime. It is possible to express the second and third terms of Equation (19) as functions of surface temperature. Procedures for accomplishing this are discussed in the next section. Once this is done, the only unknown in Equation (19) will be surface temperature. Then, Equation (19) can be solved for surface temperature.

1.2.4 Solution of Conductive Heat Flux due to Atmosphere and Soil.

Since the purpose of this paper is to study the diurnal variation of the surface temperature of Mars, we are only interested in the periodic part, not the transient part. For the periodic solution, a common form of solution is Fourier series. However, since Equation (19), a nonlinear equation, is the final equation for the temperature solution, Fourier series is not adequate. The method used here is basically due to Jaeger (1953).

If the surface temperature has period T , starting from any arbitrary point, we then divide the period T into N equal intervals. Then we assume a step function at the surface with unit temperature at the first interval and the rest of the intervals remain at zero. The periodic part of the solution for a unit amplitude can be expressed as follows:

$$\left. \begin{array}{ll} \phi(t) = 0 & t < 0 \\ \phi(t) = 1 & mT < t < mT + T_1 \\ \phi(t) = 0 & mT + T_1 < t < (m+1)T \end{array} \right\} \quad (20)$$

where T_1 is an integral multiple of $\frac{T}{N}$, and m is an integer.

By Laplace transformation, we have

$$\begin{aligned}
 \bar{\phi} &= \int_0^{\infty} e^{-pt} \phi(t) dt = \sum_{m=0}^{\infty} \int_{mT}^{(m+1)T} \phi(t) e^{-pt} dt \\
 &= \sum_{m=0}^{\infty} e^{-mpT} \int_0^T e^{-pt'} \phi(t') dt' \\
 &= \sum_{m=0}^{\infty} e^{-mpT} \int_0^T e^{-pt'} dt' .
 \end{aligned}$$

Since

$$\sum_{m=0}^{\infty} e^{-mpT} = \frac{1}{1 - e^{-pT}}$$

it follows

$$\bar{\phi} = \frac{(1 - e^{-pT_1})}{p(1 - e^{-pT})} . \quad (21)$$

Now the solution of spatial part of the Laplace transformation of Equation (14) with an assumed initial condition $\theta = 0$ and unit surface temperature is

$$\bar{\theta} = AK_0[2q(1 + \alpha z)^{1/2}/\alpha] + BI_0[2q(1 + \alpha z)^{1/2}/\alpha]$$

where I_0 , K_0 equals the modified Bessel function of the first and second kind of order zero, respectively

q equals $\left(\frac{p\rho c}{k'}\right)^{1/2}$

A, B equal functions of time.

Since θ is finite at large distances, B must be zero. Applying the boundary condition at $z=0$, one obtains

$$A = \frac{\bar{\phi}(p)}{K_0(2q/\alpha)}, \quad (22)$$

and

$$\bar{\theta} = \frac{\phi(p)}{K_0(2q/\alpha)} K_0[2q(1 + \alpha z)^{1/2}/\alpha] \quad (23)$$

(If θ_s is the amplitude at the surface, the total transformed temperature will be $\theta_s \bar{\theta}$.)

The flux due to a unit temperature $\bar{\theta}$ is

$$\bar{f}_a = -k'(1 + \alpha z) \frac{\partial \bar{\theta}}{\partial z} = (p)^{1/2} (\rho c k')^{1/2} \cdot \frac{(1 + \alpha z)^{1/2} \bar{\phi}(t) \cdot K_1[2q(1 + \alpha z)^{1/2}/\alpha]}{K_0(2q/\alpha)} \quad (24)$$

where K_1 is the modified Bessel function of the second kind of order one.

By the inversion theorem, f_a can be written as

$$f_a = \frac{(\rho c k')^{1/2} (1 + \alpha z)^{1/2}}{2\pi i} \int_{c-i\infty}^{c+i\infty} \frac{e^{pt} (1 - e^{-pT_1}) K_1[2q(1 + \alpha z)^{1/2}/\alpha]}{\sqrt{p} (1 - e^{-pT}) K_0(2q/\alpha)} dp \quad (25)$$

At the surface $z = 0$, f_a for all time t is simply

$$f_a = \frac{(\rho c k')^{1/2}}{2\pi i} \int_{c-i\infty}^{c+i\infty} \frac{e^{pt}(1 - e^{-pT_1})}{\sqrt{p}(1 - e^{-pT})} \cdot \frac{K_1 \left[\frac{2}{\alpha K_0^{1/2}} p^{1/2} \right]}{K_0 \left[\frac{2}{\alpha K_0^{1/2}} p^{1/2} \right]} dp \quad (26)$$

where $K_0 = \frac{k'}{\rho_0}$.

The integrand has a branch point at $p=0$ and simple poles at $p = \pm 2n\pi i/T$ with $n = 1, 2, \dots$. The contribution to Equation (26) from the branch point $p=0$ is

$$-\frac{\sqrt{\rho c k'}}{2\pi} e^{-\pi/2} \int_0^\infty \frac{e^{-xt}(1 - e^{xT_1}) [J_0(\lambda_0 x^{1/2}) J_1(\lambda_0 x^{1/2}) + Y_0(\lambda_0 x^{1/2}) Y_1(\lambda_0 x^{1/2})]}{\sqrt{x}(1 - e^{xT}) [J_0^2(\lambda_0 x^{1/2}) + Y_0^2(\lambda_0 x^{1/2})]} dx \quad (27)$$

where J_n, Y_n = Bessel functions of the first and second kind of order n respectively, and $\lambda_0 = \frac{2}{\alpha} (K_0)^{-1/2}$. It is seen that this quantity is the transient part of the solution of Equation (26). The contribution to Equation (26) from the residues at the poles $p = \pm \frac{2n\pi i}{T}$ would yield a series of terms with period T . The steady periodic solution would then be the sum of this series. However, instead of evaluating the residues now, let us represent this periodic solution by f_{ap} . Then the complete solution Equation (26) for all time t , containing both the periodic and transient parts, can be written as

$$f_a = f_{ap} + \frac{\sqrt{\rho c k'}}{2\pi} e^{-\pi/2} \int_0^\infty \frac{e^{-xt}(1 - e^{xT_1}) [J_0(\lambda x^{1/2}) J_1(\lambda x^{1/2}) + Y_0(\lambda x^{1/2}) Y_1(\lambda x^{1/2})]}{\sqrt{x}(1 - e^{xT}) [J_0^2(\lambda x^{1/2}) + Y_0^2(\lambda x^{1/2})]} dx \quad (28)$$

The quantity f_{ap} is the periodic solution which we are actually interested in. The second term is the transient part that will tend to be zero at $t \rightarrow \infty$. The reason we do not want to evaluate the residue to determine the periodic solution by summing the series is that the solution may converge rather slowly and clumsily. We want to write the solution in an integral form by comparing this result with another solution for the first period.

For this first period, $\bar{\phi}(t)$ becomes

$$\begin{aligned}\bar{\phi} &= \int_0^{\infty} e^{-pt} \cdot 1 \cdot dt \\ &= 1/p \quad 0 < t < T_1 \quad . \quad (29)\end{aligned}$$

and

$$\begin{aligned}\bar{\phi} &= \int_0^{\infty} e^{-pt} \cdot 1 \cdot dt \\ &= \int_0^{T_1} e^{-pt} dt \\ &= (1/p)(1 - e^{-pT_1}), \quad T_1 < t \quad . \quad (30)\end{aligned}$$

It follows then that the corresponding flux is

$$f_{a1} = -\frac{(k' \rho c e^{-\pi})^{1/2}}{2\pi} \int_0^{\infty} \frac{e^{-xt} (J_0 J_1 + Y_0 Y_1)}{\sqrt{x} (J_0^2 + Y_0^2)} dx, \quad 0 < t < T_1, \quad (31)$$

$$f_{an} = -\frac{(k' \rho c e^{-\pi})^{1/2}}{2\pi} \int_0^{\infty} \frac{e^{-xt} (1 - e^{xT_1}) (J_0 J_1 + Y_0 Y_1)}{\sqrt{x} (J_0^2 + Y_0^2)} dx, \quad T_1 < t. \quad (32)$$

where $J_n, Y_n = J_n(\lambda x^{1/2}), Y_n(\lambda x^{1/2})$, respectively. Substituting Equations (31) and (32) into Equation (28) yields

$$\therefore f_{ap1} = \frac{(k' \rho c e^{-\pi})^{1/2}}{2\pi} \int_0^{\infty} \frac{e^{-xt} (J_0 J_1 + Y_0 Y_1)}{\sqrt{x} (J_0^2 + Y_0^2)} \left[\left(\frac{1 - e^{xT_1}}{1 - e^{xT}} \right) - 1 \right] dx, \quad mT < t < mT + T_1, \quad (33)$$

and

$$f_{apn} = \frac{(k' \rho c e^{-\pi})^{1/2}}{2\pi} \int_0^{\infty} \frac{e^{-xt} (J_0 J_1 + Y_0 Y_1)}{\sqrt{x} (J_0^2 + Y_0^2)} \left[\frac{1 - e^{xT_1}}{1 - e^{xT}} \left(1 - e^{+xT_1} \right) \right] dx, \quad (34)$$

$$mT + T_1 < t < (m+1)T.$$

Now taking the average of Equation (33) in the first interval $0 < t < T_1 = T/N$, and letting $xT = \xi^2$, the average flux into the air due to a unit temperature at the surface for the indicated interval will be

$$\begin{aligned}
(f_a)_1 &= \frac{N}{T} \int_0^{T/N} f_{apl} dt = \frac{N}{\pi^{1/2}} \left(\frac{k' \rho c e^{-\pi}}{\pi T} \right)^{1/2} \int_0^{\infty} \frac{\left[\exp\left(-\frac{\xi^2}{N}\right) - 1 \right] \left[1 - \exp\left(-\frac{N-1}{N} \xi^2\right) \right]}{\xi^2 (1 - e^{-\xi^2})} \\
&\quad \frac{(J_o J_1 - Y_o Y_1)}{J_o^2 + Y_o^2} d\xi \\
mT < t < mT + T_1
\end{aligned} \tag{35}$$

in which the argument of J_n and Y_n is $\lambda_o(T)^{-1/2}$ where $()_1$ = the average flux of periodic solution at the first time interval. And similarly, for the n -th interval, it is

$$\begin{aligned}
(f_a)_n &= \frac{N}{T} \int_{\frac{n-1}{N}T}^{nT/N} f_{apn} dt \\
&= \frac{N}{\pi^{1/2}} \left(\frac{k' \rho c e^{-\pi}}{\pi T} \right)^{1/2} \int_0^{\infty} \frac{\left[\exp(-n\xi^2) - \exp\left(-\frac{n-1}{N}\xi^2\right) \right] \left[1 - \exp\left(-\frac{\xi^2}{N}\right) \right] [J_o J_1 - Y_o Y_1]}{\xi^2 (1 - e^{-\xi^2}) [J_o^2 + Y_o^2]} d\xi \\
mT + T_1 < t < (m+1)T
\end{aligned} \tag{36}$$

The argument of J_n or Y_n is again $\lambda_o(T)^{-1/2}$.

If the average amplitude of the surface temperature in the successive ℓ -th interval is θ_ℓ ($\ell = 1, 2, \dots, n$) then the average flux into the air in the n -th interval is

$$f_{an} = \sum_{\ell=1}^N \theta_\ell \phi(f_a)_{n-\ell+1} \quad . \tag{37}$$

Similarly, the solution of the average flux into the soil due to the unit surface temperature based on the differential Equation (15) for the first and n-th intervals are

$$(f_s)_1 = \bar{K}_s \frac{\partial T_s}{\partial z} = - \left(\frac{\bar{K}_s}{\pi T} \rho_s c_s \right)^{1/2} \left\{ 2N^{1/2} - \frac{2N}{\pi^{1/2}} \int_0^\infty \frac{\left[1 - \exp\left(-\frac{\xi^2}{N}\right) \right] \left[\exp\left(-\frac{N-1}{N} \xi^2\right) - e^{-\xi^2} \right]}{\xi^2 (1 - e^{-\xi^2})} d\xi \right\}$$

for $mT < t < mT + T_1$ (38)

and

$$(f_s)_n = - \left(\frac{\bar{K}_s \rho_s c_s}{T_s \pi} \right)^{1/2} \left\{ 2N^{1/2} [n^{1/2} - 2(n-1)^{1/2} - (n-2)] - \frac{2N}{\pi^{1/2}} \int_0^\infty \frac{\exp\left(-\frac{n-1}{N} \xi^2\right) \left[1 - \exp\left(-\frac{\xi^2}{N}\right) \right] \exp\left(-\frac{N-1}{N} \xi^2\right) e^{-\xi^2}}{\xi^2 (1 - e^{-\xi^2})} d\xi \right\}$$

($n = 2, 3, \dots, n$) ,

$$\text{for } mT + T_1 < t < (m+1)T \quad . \quad (39)$$

If the average amplitude of the surface temperature in the successive l -th interval is T_{sl} ($l = 1, 2, \dots, n$), then the average flux into the soil is

$$F_{sn} = \sum_{\ell=1}^N T_{s\ell} (f_s)_{n-\ell+1} \quad (40)$$

Then substituting Equations (37) and (40) into Equation (19) and using Equation (17), one obtains

$$(1-\alpha)\sigma T_{s\ell}^4 + \sum_{\ell=1}^N T_{s\ell} (f_a)_{n-\ell+1} + \sum_{\ell=1}^N T_{s\ell} (f_s)_{n-\ell+1} - \mu I_{\infty} (\sin \phi \sin \delta + \cos \phi \cos \delta \cos \psi)_{\ell} = 0, \\ \ell = 1, \dots, n \quad (41)$$

The last term can be computed for different latitudes, solar declinations and hour angles. During the night this term should vanish. For special cases, at the equator ($\phi = 0$), for a given date, the last term of Equation (41) may be written as

$$\frac{1-A}{r^2} S \cos 2\pi \frac{t}{T} = \begin{cases} \frac{1-A}{r^2} S \cos 2\pi \frac{t}{T}, & \frac{T}{4} < t < \frac{3}{4} T, \\ 0, & \text{otherwise,} \end{cases} \quad (42)$$

where A = planetary albedo

S = solar constant at Earth's distance from sun,

r = distance to the sun in astronomical units.

Equation (41) is actually a set of N quadratic algebraic equations, which can be solved numerically by hand computations or electronic computer. Such computations are planned for the next quarter.

1.3 INTERHEMISPHERIC TRANSPORT OF WATER VAPOR AND THE MARTIAN ICE CAPS

1.3.1 Introduction. One of the fundamental problems of the meteorology of Mars concerns its ice caps. The amount of water vapor in the Martian atmosphere is about $10^{-3} \text{ g cm}^{-2}$. The thickness of the ice caps is of the order of 1 cm. During the course of the Martian year, as one polar ice cap forms, the other sublimates and completely disappears. The amount of water vapor in the atmosphere, even if it were all to condense, could not account for the formation of the ice caps. Thus, it has been suggested that, as one ice cap melts, the water vapor released into the atmosphere is transported to the opposite pole, where it condenses. At any one time, then, most of the Martian water vapor is located in the polar caps. During each Martian year, there is an atmospheric shuttling of water vapor from one pole to the other.

There are two possible atmospheric mechanisms that might accomplish the required transport: a mean meridional velocity and large-scale atmospheric diffusion. The rate of transport from one pole to the other is probably greatest during the equinoctial seasons, when one cap is melting and the other is forming. During these seasons, the Martian temperatures are probably highest at the equator and lowest at the poles. With such a temperature distribution, a meridional circulation system would be characterized by equatorward motion at the surface and poleward motion aloft. The mean meridional velocity pattern required to explain the ice cap formation is characterized by a surface flow from the melting polar cap to the forming polar cap. Obviously, the required flow is not

compatible with the probable flow pattern during the equinoctial seasons. As the solstice approaches, the summer pole heats up and may become the hottest point on the planet. A meridional circulation system at this time would be characterized by flow from the summer pole to the winter pole at upper levels and the reverse near the surface. Again, the required flow -- from summer to winter pole near the surface -- is not compatible with the probable Martian flow pattern. Thus, a mean meridional velocity does not appear to be a satisfactory explanation of the interhemispheric transport of water vapor. We have begun to investigate whether the other possible explanation -- large-scale atmospheric diffusion -- is reasonable, and to determine the values of the large-scale diffusion coefficients required to accomplish the required transports of water vapor.

In the Earth's atmosphere, large-scale latitudinal transports of heat, momentum, and trace substances, such as water vapor, are accomplished by large-scale eddy diffusion processes. There are indications that within an individual hemisphere thorough mixing of a trace constituent can occur over time periods of the order of months (Junge, 1962). Interhemispheric mixing times, on the other hand, have variously been estimated to be from 0.9 years to 4 years (Junge, 1963). For the Martian ice cap cycle, an interhemispheric mixing time of the order of one Earth year is required, since a complete ice cap cycle is completed in about two Earth years. Such a mixing time does not seem improbable when compared with the above values for Earth.

In the following discussion, we describe a simple global diffusion model, in which water vapor is released into the atmosphere by the melting of a north polar ice cap on Mars. With reasonable values for a large-scale diffusion coefficient, we calculate the latitudinal variation of water vapor as a function of time to see how rapidly the water vapor can proceed from one pole to the other. In future models, we plan to include both a source (the melting polar cap) and a sink (the forming polar cap) in a more realistic, periodic model of the seasonal variations of atmospheric water vapor.

1.3.2 Discussion. Several models of the transport of water vapor on Mars are being developed. In these models, the transport of water vapor is entirely due to large-scale meridional diffusion, with a diffusion coefficient, K , independent of latitude.

The concentration of water vapor, $q(\mu, t)$ (grams/cm²), where $\mu = \sin \theta$, θ being the angle of latitude, and the sources and sinks, $Q(\mu, t)$ (grams/cm²/sec), are related by the following equation:

$$\frac{\partial q}{\partial t} = \frac{K}{2a} \frac{\partial}{\partial \mu} \left[(1 - \mu^2) \frac{\partial q}{\partial \mu} \right] + Q, \quad (43)$$

where a is the radius of the planet.

Since the set of Legendre polynomials, $P_n(\mu)$ satisfies the equation

$$\frac{\partial}{\partial \mu} \left[(1 - \mu^2) \frac{\partial P_n(\mu)}{\partial \mu} \right] = -n(n+1) P_n(\mu), \quad (44)$$

$q(\mu, t)$, and $Q(\mu, t)$ are expanded in Legendre polynomials:

$$q(\mu, t) = \sum_{n=0}^{\infty} q_n(t) P_n(\mu) \quad (45)$$

$$Q(\mu, t) = \sum_{n=0}^{\infty} Q_n(t) P_n(\mu) \quad , \quad (46)$$

where the coefficients, q_n and Q_n , are functions of time. Taking the Laplace transform of $q(\mu, t)$, $Q(\mu, t)$, and $\frac{\partial q}{\partial t}$, we get

$$\bar{q}(\mu, p) = \sum_{n=0}^{\infty} \bar{q}_n(p) P_n(\mu) \quad (47)$$

$$\bar{Q}(\mu, p) = \sum_{n=0}^{\infty} \bar{Q}_n(p) P_n(\mu) \quad (48)$$

$$\mathcal{L} \left\{ \frac{\partial q}{\partial t} \right\} = \sum_{n=0}^{\infty} [p \bar{q}_n(p) - q_n(0)] P_n(\mu) \quad . \quad (49)$$

In (49) the set, $\{q_n(0)\}$, are the coefficients in the expansion of $q(\mu, 0)$, the initial concentration of water vapor. Inserting Equations (47), (48), and (49) into Equation (43), we get

$$\sum_{n=0}^{\infty} [p \bar{q}_n(p) - q_n(0) + (n)(n+1) \frac{K}{2} \bar{q}_n(p) - \bar{Q}_n(p)] P_n(\mu) = 0 \quad (50)$$

which gives the following equation relating \bar{Q}_n and \bar{q}_n :

$$\bar{q}_n(p) = \frac{[\bar{Q}_n(p) + q(0)]}{p + \frac{K}{2} (n)(n+1)} \quad (51)$$

To obtain the inverse transform, we use the convolution theorem,

$$\mathcal{L} \left\{ \int_0^t f(x)g(t-x)dx \right\} = \bar{f}(p) \cdot \bar{g}(p) \quad (52)$$

where $\bar{f}(p) = \bar{Q}_n(p)$, and

$$\bar{g}(p) = \frac{1}{p + \frac{K}{2a} (n)(n+1)}$$

Thus, the equation relating the source coefficients and the concentration coefficients is:

$$q_n(t) = \int_0^t Q_n(x) \exp\left(-\frac{K}{2a}(n)(n+1)(t-x)\right) dx + q_n(0) \exp\left(-\frac{K}{2a}(n)(n+1)t\right) \quad (53)$$

In the first model, the source is due to the sublimation of the north polar cap. The cap has a constant thickness of 1 cm from 60° to 90° , and it is assumed that all the ice vaporizes at the instant $t=0$. The simplest approach to this problem is to consider Equation (43) as an initial value equation where the source, Q , is zero for all time, and at time $t=0$, the initial concentration of water vapor $q(\mu,0)$, is 1 gram per square centimeter from 60° to 90° and zero elsewhere. Thus, Equation (53) gives

$$q_n(t) = q_n(0) \exp\left(-\frac{K}{2a}(n)(n+1)t\right) \quad (54)$$

where $q_n(0)$ is the n -th coefficient in the expansion of $q(\mu,0)$.

Sample computations were made by expanding $q(\mu, 0)$ in the first nine Legendre polynomials, P_0, P_1, \dots, P_8 , and obtaining the corresponding coefficients $q_n(t)$, for $t=0$, 1 month, 2 months, ..., 6 months (these are Earth months). Figure 3 is a graph of $q(\mu, t)$ as a function of μ for these times, and for $K = 10^{10} \text{ cm}^2/\text{sec}$. It is seen that the curve, $q(\mu, 0)$, is not fitted too well with the first nine Legendre polynomials. However, due to the exponential factor in Equation (54), these perturbations become negligibly small in the remaining curves. It can be seen that with this model water vapor first arrives at the south pole during the second month after the release of water vapor from the northern hemisphere ice cap. By the end of six months, the water vapor is evenly distributed throughout the planet.

In the second model, a more realistic source function is used. In this model, at the instant $t=0$, only the ice at the edge of the north polar cap vaporizes. Then, as time goes on, the ice cap recedes toward the north pole as the perimeter of the cap continually sublimates and gives off water vapor to the atmosphere. The source function in this model is given by

$$Q(\mu, t) = \begin{cases} A[1 - \cos \frac{2\pi}{\Delta\mu} (\mu - \mu_0 - vt)] & , \mu_0 + vt \leq \mu \leq \mu_0 + vt + \Delta\mu \\ 0 & , \text{otherwise} \end{cases}$$

where A is the amplitude, μ_0 is the sine of the latitude where sublimation begins at the instant $t=0$, $\Delta\mu$ is the width of the source function, and v is the velocity of the recession of the ice cap toward the pole. Numerical computations with this model will be completed in the near future.

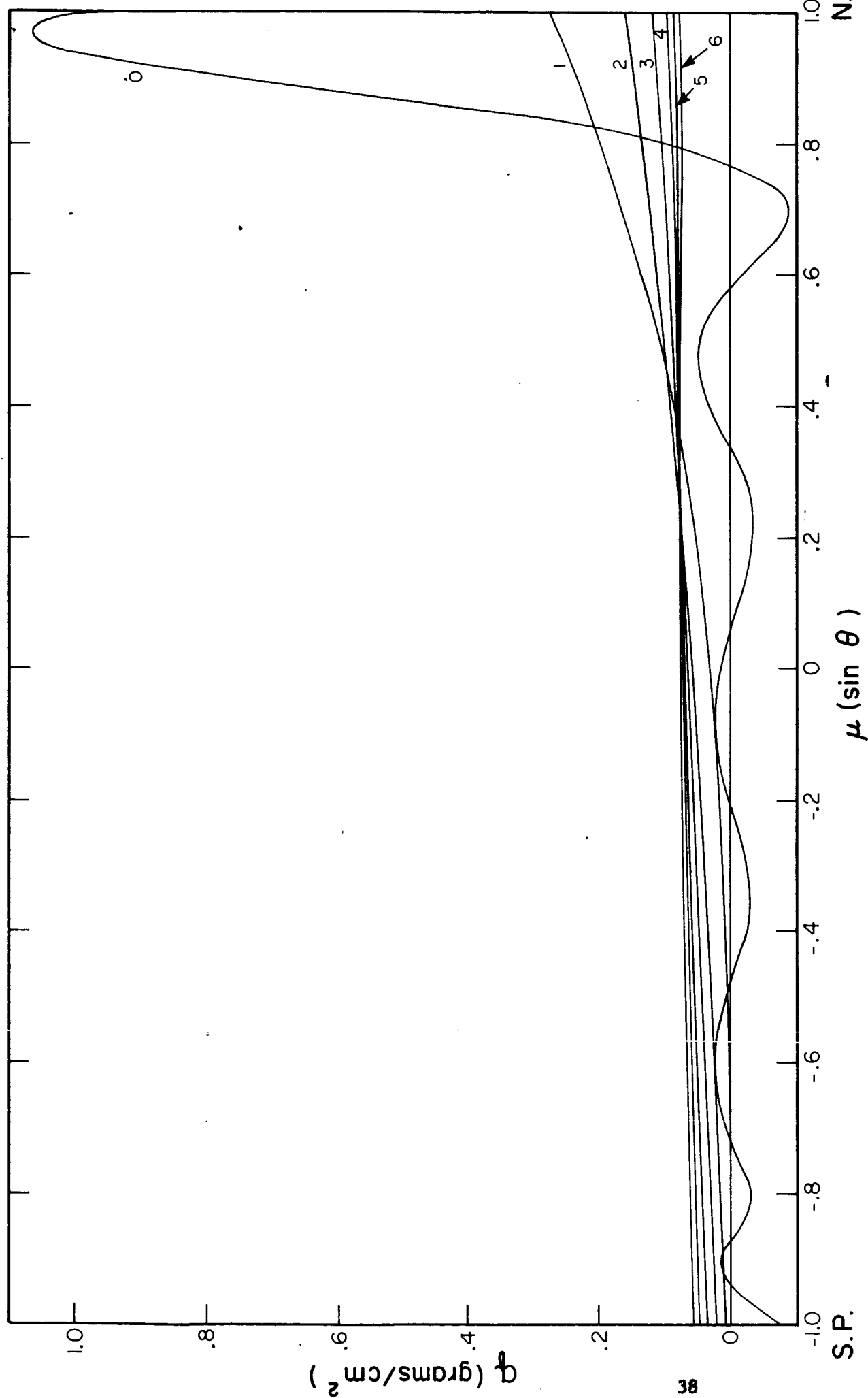


Figure 3. Latitudinal distribution of water vapor as a function of time in months after an instantaneous release in the north polar area.

1.4 A COMPARISON OF ZONAL WIND VELOCITIES ON MARS AND EARTH

Gifford (1964) has summarized information on Martian yellow clouds that displayed movement. He divided Martian yellow cloud occurrences into two groups - those that were observed on the disc of Mars and those that were observed as terminator projections. Gifford suggests that the first group of clouds is located near the surface of Mars while the second group is located higher in the atmosphere. Gifford also presents information on observed drifts of these clouds. From these data, we have computed average zonal velocities as a function of latitude for the projection clouds. In Figure 4, we compare these data with average zonal velocities observed in the Earth's atmosphere. The values for the Earth's atmosphere are based upon an average of the mean zonal velocities presented by Obasi (1963) for southern hemisphere winter and summer. Obasi's values are derived from observations between 850 mb and 50 mb during 1958.

It must be realized that the number of Martian observations is extremely small - about 25. Nevertheless, the similarity between the zonal velocities in the two atmospheres is quite interesting. On both Mars and Earth the zonal west wind increases with latitude to a maximum at middle latitudes and then decreases towards the poles. This comparison suggests that the circulation patterns of the two planets may be quite similar. There is, however, an anomalous decrease in zonal wind on Mars between 20 and 40° latitude. This may be due to the lack of representative data for Mars, or it may be real.

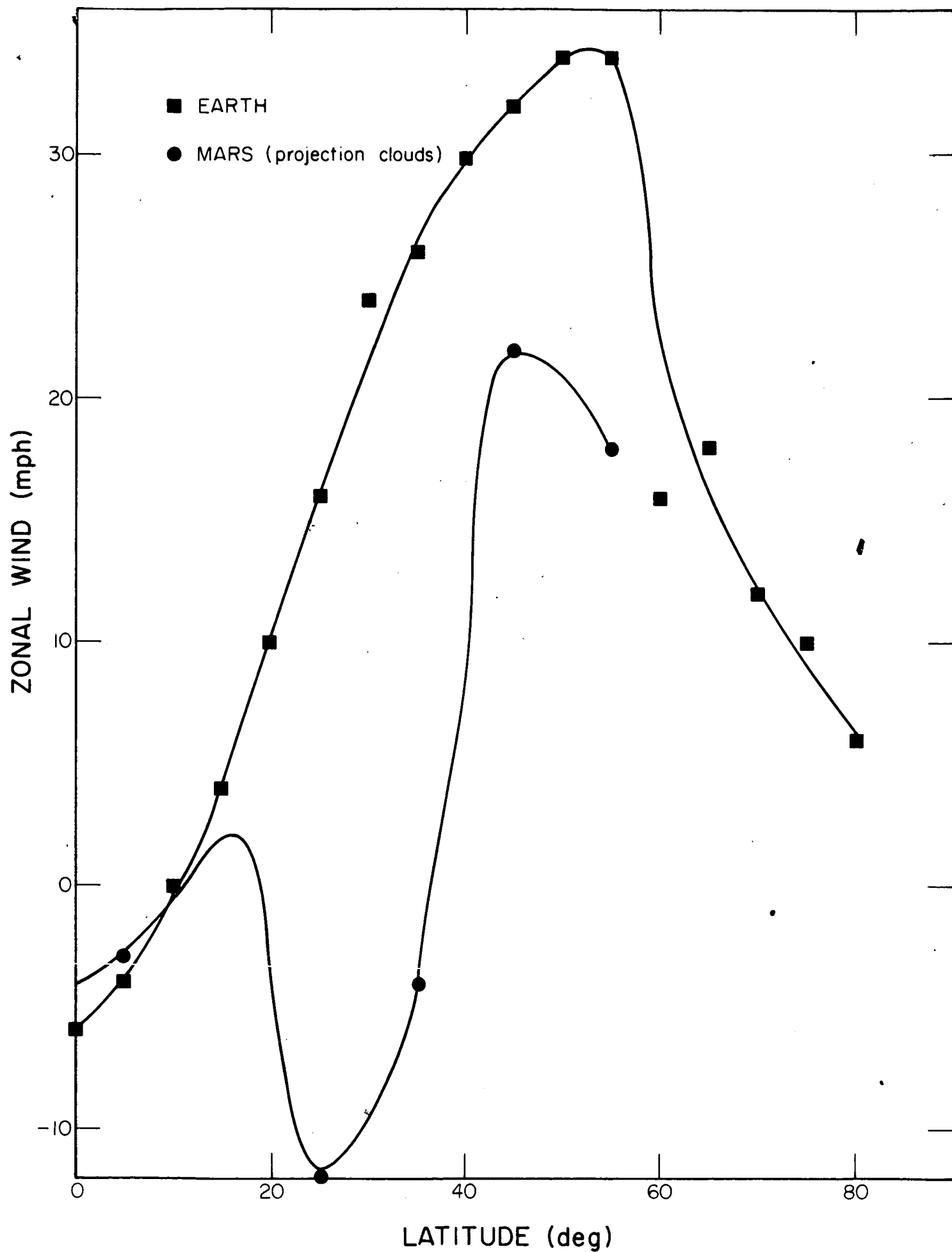


Figure 4. Comparison of latitudinal variation of mean zonal winds on Mars and Earth.

There is one other problem in connection with the interpretation of the projection cloud drifts. We have assumed that the cloud drifts are representative of atmospheric wind velocities. Another interpretation is possible. It may be that the cloud drifts represent motions of entire cloud systems and, thus, velocities derived from such drifts may refer to storm translation speeds rather than atmospheric winds.

SECTION 2
METEOROLOGY OF VENUS

2.1 ATMOSPHERIC CIRCULATION IN THE VENUSIAN ATMOSPHERE

The convective model of the compressible atmosphere proposed in the previous Final Report (Contract No. NASw-975) was developed in order to study the general circulation of the Venusian atmosphere. Unsuccessful attempts were made to solve the resulting sixth order linear ordinary differential equation by finite difference techniques. Present techniques for solving a difference equation of order higher than two usually lead to numerical solutions with rather large errors. Apparently, these techniques failed completely in our attempts to solve the sixth-order differential equation. A new approach to our problem of convection in a compressible atmosphere is developed here. Instead of using the finite difference technique, we assume a set of Fourier series solutions for dependent variables. The coefficients of the terms of the Fourier series will be finally determined by a linear algebraic method.

Instead of obtaining the solution for the sixth-order differential equation (94) or (95) of the previous Final Report (Contract No. NASw-975), we retain equations (87) and (88) in their original form and combine (85), (86) and (89) to eliminate $\hat{\rho}$ and \hat{p} . This process leads to the following equations:

$$\hat{L}\hat{T} = \hat{\phi}\hat{w} \quad , \quad (55)$$

$$b\hat{u} = \left(\frac{1}{H} - D \right) \hat{w} , \quad (56)$$

$$\frac{g}{\beta} \hat{T} = \nu \rho_o(z) L \hat{w} - \frac{\nu}{b} [D \rho_o(z)] L \hat{u} - \frac{\nu}{b} \rho_o(z) D L \hat{u} + \frac{g \alpha \nu}{\beta b} \rho_o(z) L \hat{u} , \quad (57)$$

where

$$L = \frac{d^2}{dz^2} - \sigma b^2 ,$$

$$D = \frac{d}{dz}$$

$$\phi = \frac{1}{\kappa_v} \left[\frac{\partial T_o}{\partial z} + \frac{(\lambda-1) T_o}{H(z)} \right] = \text{constant} ,$$

$$\rho_o(z) = \frac{p_s \gamma \kappa_*}{g T_s} \left(1 - \frac{\gamma z}{T_s} \right)^{\frac{1-\kappa_*}{\kappa_*}} ,$$

$$H(z) = \frac{\kappa_*}{\kappa_* - 1} \frac{T_s}{\gamma} \left(1 - \frac{\gamma z}{T_s} \right) ,$$

(for an explanation of other notations, please refer to the Final Report, NASw-975).

Now use the transformation for z

$$z = \frac{h}{\pi} z_* ,$$

where h = the depth of the atmospheric system. Then Equations (55), (56) and (57) become

$$L_* \hat{T} = \phi_* \hat{w} , \quad (58)$$

$$b_* \hat{u} = \left(\frac{1}{H_*} - D_* \right) \hat{w} , \quad (59)$$

$$\left(\frac{h}{\pi} \right)^2 \frac{g}{\beta} \hat{T} = \nu \rho_{o*} L_* \hat{w} - \frac{\nu}{b_*} [D_* \rho_{o*}] L_* \hat{u} - \frac{\nu}{b_*} \rho_{o*} D_* L_* \hat{u} + \frac{g \alpha \nu}{\beta b_*} \left(\frac{h}{\pi} \right) \rho_{o*} L_* \hat{u} , \quad (60)$$

where

$$L_* = \frac{d^2}{dz_*^2} - \sigma b_*^2 ,$$

$$D_* = \frac{d}{dz_*} ,$$

$$b_* = \frac{bh}{\pi} ,$$

$$\phi_* = \phi \left(\frac{h}{\pi} \right)^2 ,$$

$$\rho_{0*} = \frac{p_s \gamma K_s}{g T_s} \left(1 - \frac{\gamma h}{T_s \pi} z_* \right)^{\frac{1-K_*}{K_*}} ,$$

$$H_* = \frac{K_*}{K_*-1} \frac{T_s \pi}{\gamma h} \left(1 - \frac{\gamma h}{T_s \pi} z_* \right) .$$

Since the boundary conditions for \hat{u} and \hat{w} are zero at $z_* = 0$ and $z_* = \pi$, it is natural to assume the solutions for \hat{u} and \hat{w} in Fourier sine series as

$$\hat{u} = \frac{2}{\pi} \sum_{l=1}^{\infty} u_l \sin l z_* , \quad (61)$$

and

$$\hat{w} = \frac{2}{\pi} \sum_{m=1}^{\infty} w_m \sin m z_* . \quad (62)$$

The boundary conditions for T are somewhat different, i.e.

$$\hat{T} = T_g , \quad \text{at} \quad z_* = 0 ,$$

and

$$\hat{T} = 0 , \quad \text{at} \quad z_* = \pi .$$

It seems that a sine series would not be very adequate for the form \hat{T} in this case since the sine series will not yield the correct boundary condition at $z_* = 0$. However, assuming the solution of T as a sine series in the domain within the boundaries is quite legitimate. Although the sine series would converge rather slowly near the lower boundary, a representative solution can be obtained close to the lower boundary if enough terms are included. The boundary condition for \hat{T} at the lower boundary can be introduced into the solution by the following method.

If we substitute (62) into (58), multiply both sides of Equation (58) by $\sin mz_*$, and integrate with respect to z_* from 0 to π , then we have

$$\int_0^\pi \frac{d^2}{dz_*^2} \hat{T} \sin mz_* dz_* - \sigma b_*^2 \int_0^\pi \hat{T} \sin mz_* dz_* = \phi_* w_m . \quad (63)$$

Now, integrating by parts the first term on the left hand side and using the boundary condition $T = 0$ at $z_* = \pi$ and $T_m = T_g$ at $z = 0$ yields

$$+ mT_g + m^2 \int_0^\pi \hat{T} \sin mz_* dz_* . \quad (64)$$

Assuming

$$\hat{T} = \frac{2}{\pi} \sum_{n=1}^{\infty} T_n \sin nz_* , \quad (65)$$

and substituting (65) and (64) into (63), one obtains

$$mT_g + m^2(1 + \sigma b_*^2)T_m = \phi_* w_m ,$$

or

$$T_m = \frac{\phi_*}{m^2(1 + \sigma b_*^2)} w_m - \frac{T_g}{m(1 + \sigma b_*^2)} . \quad (66)$$

Now substituting (61) and (62) into (59) and multiplying by $\sin lz_*$ and integrating with respect to z_* from 0 to π , we obtain

$$u_\ell = \frac{2}{b_*\pi} \sum_{m=1}^{\infty} w_m \int_0^{\pi} \frac{1}{H_*} \sin mz_* \sin lz_* dz_* . \quad (67)$$

Similarly, substituting (61) and (62) into (60), multiplying by $\sin nz_*$, and integrating with respect to z_* from 0 to π , we obtain

$$\begin{aligned} T_n = & \frac{2\beta v}{g\pi} \left(\frac{\pi}{h} \right)^2 \left\{ \sum_{m=1}^{\infty} \int_0^{\pi} L_*(w_m \sin mz_*) \rho_{o*} \sin nz_* dz_* \right. \\ & - \frac{1}{b_*} \sum_{\ell=1}^{\infty} \int_0^{\pi} (D_* \rho_{o*}) L_*(u_\ell \sin lz_*) \sin nz_* dz_* \\ & - \frac{1}{b_*} \sum_{\ell=1}^{\infty} \int_0^{\pi} D_* L_*(u_\ell \sin lz_*) \rho_{o*} \sin nz_* dz_* \\ & \left. + \frac{g\alpha}{\beta b_*} \left(\frac{h}{\pi} \right) \sum_{\ell=1}^{\infty} \int_0^{\pi} L_*(u_\ell \sin lz_*) \rho_{o*} \sin nz_* dz_* \right\} . \quad (68) \end{aligned}$$

The third term of the right hand side of (68) contains a third derivative of u or $\sin lz_*$ with respect to z_* under the sign of integration. It is worthwhile to mention here that we cannot take the third derivative of $\sin lz_*$ directly, for we have no knowledge of d^2u/dz_*^2 at the boundaries.

Instead we must integrate the third derivative once. Then the third term on the right hand side of (68) becomes

$$\begin{aligned}
 & -\frac{1}{b_*} \sum_{\ell=1}^{\infty} \int_0^{\pi} \frac{d}{dz_*} L_*(u_{\ell} \sin \ell z_*) \rho_{0*} \sin n z_* dz_* = -\frac{1}{b_*} \sum_{\ell=1}^{\infty} u_{\ell} (\ell^2 + \sigma b_*^2) \cdot \\
 & \cdot \int_0^{\pi} \frac{d\rho_{0*}}{dz_*} \sin n z_* \sin \ell z_* dz_* - \frac{1}{b_*} \sum_{\ell=1}^{\infty} u_{\ell} (\ell^2 + \sigma b_*^2) \int_0^{\pi} n \rho_{0*} \cos n z_* \sin \ell z_* dz_*
 \end{aligned} \quad (69)$$

After substituting (69) into (68) and canceling out the second term of (68) with the first term of (69), one obtains

$$\begin{aligned}
 T_n = \frac{2\beta v}{g\pi} \left(\frac{\pi}{h} \right)^2 \left\{ - \sum_{m=1}^{\infty} w_m (m^2 + \sigma b_*^2) \int_0^{\pi} \rho_{0*} \sin m z_* \sin n z_* dz_* \right. \\
 - \frac{1}{b_*} \sum_{\ell=1}^{\infty} u_{\ell} (\ell^2 + \sigma b_*^2) \cdot n \cdot \int_0^{\pi} \rho_{0*} \cos n z_* \sin \ell z_* dz_* \\
 \left. - \frac{g\alpha}{\beta b_*} \left(\frac{h}{\pi} \right) \sum_{\ell=1}^{\infty} u_{\ell} (\ell^2 + \sigma b_*^2) \int_0^{\pi} \rho_{0*} \sin n z_* \sin \ell z_* dz_* \right\}, \quad (70)
 \end{aligned}$$

or, in a concise form,

$$T_n = \frac{2\beta v}{g\pi} \left(\frac{\pi}{h} \right)^2 \left\{ - \sum_{m=1}^{\infty} w_m h(m, n) - \frac{1}{b_*} \sum_{\ell=1}^{\infty} u_{\ell} g(\ell, n) \right\}, \quad (71)$$

where

$$h(m, n) = (m^2 + \sigma b_*^2) \int_0^{\pi} \rho_{0*} \sin m z_* \sin n z_* dz_*, \quad (72)$$

and

$$g(\ell, n) = (\ell^2 + \sigma b_*^2) \cdot n \cdot \int_0^\pi \rho_{0*} \cos n z_* \sin \ell z_* dz_* - \frac{g\alpha}{\beta} \left(\frac{h}{\pi} \right) (\ell^2 + \sigma b_*^2) \int_0^\pi \rho_{0*} \sin n z_* \sin \ell z_* dz_* . \quad (73)$$

Substituting (66) and (67) into (71) one obtains

$$- \frac{2\beta\gamma}{g\pi} \left(\frac{\pi}{h} \right)^2 \left\{ + \sum_{m=1}^{\infty} w_m h(m, n) + \left(\frac{2}{b_*^2 \pi} \right) \sum_{\ell=1}^{\infty} \sum_{m=1}^{\infty} w_m \left[\int_0^\pi \frac{1}{H_*(z_*)} \cdot \sin m z_* \sin \ell z_* dz_* \right] g(\ell, n) \right\} - \frac{\phi_* w_n}{n(1 + \sigma b_*^2)} = \frac{T_g}{n(1 + \sigma b_*^2)} . \quad (74)$$

If we truncate the Fourier series at the 30th term ($\ell, m, n = 1, 2, \dots, 30$), then a 30×30 matrix will be eventually solved in order to obtain w_m ($m = 1, 2, \dots, 30$). Thus, the vertical velocity can be obtained as a sine series with determined coefficients. Once the vertical velocity is obtained, one can obtain the temperature and horizontal velocity from Equations (62) and (63) respectively.

Numerical evaluation of the matrices is planned.

2.2 THE COMPOSITION OF THE VENUSIAN CLOUDS

2.2.1 Introduction. From an analysis of the near infrared reflection spectrum of the Venusian clouds, Bottema et al. (1964) have concluded that

the clouds are composed of ice crystals. Arguments against ice (or water) clouds on Venus have been given by Sagan and Kellogg (1963) and, more recently, by Chamberlain (1965). These arguments are based upon a comparison of the water vapor mixing ratio derived from the observations of water vapor amounts above the Venusian clouds and the required saturation mixing ratio for condensation at the observed cloud-top temperatures. Such a comparison indicates that the water vapor mixing ratios are below those required for condensation. However, the computations by Sagan and Kellogg, and Chamberlain, are based upon the assumption that the water vapor mixing ratio is constant with altitude above the clouds. This is not necessarily the case. In the earth's atmosphere, for example, the water vapor mixing ratio generally decreases with altitude. In this section, we investigate whether condensation can occur at the cloud-tops, if the water vapor mixing ratio decreases with altitude at rates comparable to those in the earth's atmosphere.

2.2.2 Discussion. The water vapor mixing ratio is defined as the ratio of the density of water vapor to the density of the dry atmosphere containing the water vapor. However, to a high degree of approximation, it can be represented as

$$w = \frac{\rho_v}{\rho} \quad (75)$$

where w is the mixing ratio, ρ_v is the water vapor density, and ρ is the total density of the atmosphere. Spectroscopic observations yield the

total amount of water vapor above a given reflecting level, which is equivalent to

$$\int_z^{\infty} \rho_v dz ,$$

with units of $g\text{ cm}^{-2}$. The results of several such observations are shown in the second column of Table 1. It may be noted that Bottema et al.(1964) give two different values based upon two different reflecting levels, while Spinrad (1962) gives only an upper limit to the possible amount of water vapor. If it is assumed that the water mixing ratio is constant with altitude, its value can be obtained as follows. From the definition of mixing ratio

$$\rho_v = w\rho \quad . \quad (76)$$

Integrating both sides with respect to height, and using the hydrostatic equation, we have

$$\int_z^{\infty} \rho_v dz = w \int_z^{\infty} \rho dz = \frac{w}{g} p_z \quad (77)$$

where p_z is the pressure at the reflecting level, and g is the gravitational acceleration. The mixing ratio can then be written as

$$w = \int_z^{\infty} \rho_v dz / (p_z/g) \quad . \quad (78)$$

Table 1 indicates the results of such computations in the column labeled $k = 0$. The saturation mixing ratio is

$$w_s = \frac{m_v}{m} \left(\frac{e_s}{p} \right)_z \quad (79)$$

TABLE 1

Cloud-top water vapor mixing ratios and saturation mixing ratios computed for various cases.

Investigator	$\int \rho_v dz$ (g/cm ²)	Presumed Reflecting Level (mb)	k=0	w_0 k=0.375	k=0.56	w_s
Spinrad (1962)	$< 7 \times 10^{-3}$	8,000	$< 10^{-5}$ to 10^{-6}			
Dollfus (1963)	1×10^{-2}	90	1×10^{-4}	3.8×10^{-4}	5.3×10^{-4}	1.15×10^{-3}
		600	1.5×10^{-5}	5.8×10^{-5}	8.0×10^{-5}	1.7×10^{-4}
Bottema et al (1964)	2.22×10^{-2} 5.2×10^{-3}	90	2.2×10^{-4}	8.5×10^{-4}	1.2×10^{-3}	1.15×10^{-3}
		600	7.7×10^{-5}	3.0×10^{-5}	4.2×10^{-5}	1.7×10^{-4}

where m_v/m is the ratio of the molecular weight of water vapor to the molecular weight of the Venusian atmosphere, and e_s is the saturation vapor pressure. If we assume the molecular weight of the Venusian atmosphere is equal to that of nitrogen, $m_v/m = 0.64$. If the cloud-top temperature is 235K, then $e_s = 0.16$ mb, and $w_s = 1.15 \times 10^{-3}$ for a cloud-top pressure of 90 mb and 1.7×10^{-4} for a cloud-top pressure of 600 mb. It can be seen from Table 1 that the constant mixing ratios are much less than the saturation mixing ratios. On the basis of similar computations, Sagan and Kellogg (1964) and Chamberlain (1965) have questioned the aqueous nature of the Venusian clouds.

Gutnick (1962) has analyzed the variation of water vapor mixing ratio with altitude at middle latitudes in the earth's atmosphere. In the troposphere, the average mixing ratio decreases logarithmically with altitude. Such a decrease can be represented by

$$\frac{d \ln w}{dz} = -k \quad . \quad (80)$$

Gutnick's data indicate that the average value of k is about 0.375 km^{-1} between the surface and 7 km, and about 0.56 km^{-1} between 7 km and 14 km.

If we assume similar variations of mixing ratio with altitude above the Venusian clouds, keeping the total water vapor amount consistent with the observations, what mixing ratios would be obtain at the cloud-top? We have

$$w = w_0 e^{-kz} \quad (81)$$

for the variation of mixing ratio above the clouds. For constant mixing ratio, $k = 0$. The variation of water vapor density with altitude can then be written as

$$\rho_v = \rho \left(\frac{\rho_v}{\rho} \right)_0 e^{-kz} \quad (82)$$

where the subscript zero refers to the cloud-top. The variation of atmospheric density with altitude is

$$\rho = \rho_0 e^{-z/H} \quad (83)$$

where H is the scale height. For a nitrogen atmosphere with a temperature of 235K and $g = 880 \text{ cm/sec}^2$, $H = 7.9 \text{ km}$. Substituting (83) into (82), we have

$$\rho_v = (\rho_v)_0 e^{-(0.127+k)z} \quad (84)$$

The integral of (84) with respect to height must be equal to the observed total amount of water vapor above the cloud,

$$\int_0^{\infty} \rho_v dz = (\rho_v)_0 \int_0^{\infty} e^{-(0.127+k)z} dz \quad (85)$$

Integrating the right hand side of (85) and solving for $(\rho_v)_0$, we find

$$(\rho_v)_0 = (0.127 + k) \int_0^{\infty} \rho_v dz \quad (86)$$

The mixing ratio at the cloud top can then be obtained from $(\rho_v/\rho)_0$, where ρ_0 is computed from

$$\rho_0 = \frac{mp}{R^* T} \quad (87)$$

where p and T are the pressure (90 mb and 600 mb) and temperature (235K) at the cloud top, and R^* is the universal gas constant. Cloud-top mixing ratios computed in this manner are shown in Table 1 for the $k = 0.375$ and $k = 0.56$. It is apparent from Table 1 that these mixing ratios are much closer to the required saturation mixing ratios and, in fact, saturation would occur for the data of Bottema et al. (1964) in the 90 mb case for $k = 0.56$.

Thus, at least for the observations of Bottema et al. (1964), the observed water vapor amounts are compatible with an ice crystal cloud if the cloud-top pressure is about 90 mb, the cloud-top temperature is 235K or less, and the water vapor mixing ratio decreases with altitude at a rate comparable to that in the earth's upper troposphere. There is no reason to believe that the assumption of a constant mixing ratio above the cloud is better than the assumption of a logarithmic decrease. In fact, a better case can be made for the assumption of a logarithmic decrease since, if the clouds are composed of water substance, the variation of mixing ratio with altitude might be similar to that observed above terrestrial clouds. A reasonable estimate of such a variation is the average value of the upper tropospheric variation of mixing ratio in the earth's atmosphere. As indicated above, this value leads, under certain conditions, to cloud-top mixing ratios compatible with the presence of clouds composed of water substance. Thus, we may conclude that compatibility between the observed water vapor amounts and the presence of water clouds on Venus can be achieved under certain conditions. Or, put another way, the observed water vapor amounts, at the present state of our knowledge are not incompatible with the presence of water clouds on Venus.

REFERENCES

- Arking, A. 1963: Non-grey planetary atmospheres. Mem. Soc. R. Sci., Liege, 5, 180-189.
- Bottema, M., W. Plummer, and J. Strong, 1964: Water vapor in the atmosphere of Venus. Astroph. J., 139, 1021-1022.
- , Plummer, W., J. Strong, and R. Zander, 1964: Composition of the clouds of Venus. Astroph. J., 140, 1640-1641.
- Chamberlain, J.W., 1965: The atmosphere of Venus near her cloud tops. Astroph. J., 141, 1184-1205.
- Coblentz, W.W., and Lampland, C.O., 1923: Measurements of planetary radiation. Lowell Obs. Bull., No. 85.
- Dollfus, A., 1963: Observation of water vapor on the planet Venus. Compt. Rend., 256, 3250-3253.
- Estoque, M.A., 1962: A numerical model of the atmospheric boundary layer. Scientific Report No. 2, Contract No. AF19(604)-7484. Hawaii Institute of Geophysics, University of Hawaii.
- Fritz, S., 1951: Solar radiant energy and its modification by the earth and its atmosphere. Compendium of Meteorology, American Meteorological Society, Boston, 13-33.
- Gifford, F., 1956: The surface - temperature climate of Mars. Astrophys. J., 123, 154-161.
- , 1964: A study of Martian yellow clouds that display movement. Monthly Weather Review, 92, 435-440.
- Goody, R.M., 1957: The atmosphere of Mars. Weather, 12, 3-15.
- Gutnick, M., 1962: Mean annual mid-latitude moisture profiles to 31 km. Air Force Surveys in Geophysics 147, AFCRL, 30pp.
- Haurwitz, B., 1936: The daily temperature period for a linear variation of the Austausch coefficient. Trans. R. Soc. Canada, 30, Sec. 3.
- , 1961: Thermally driven circulations in a rotating fluid system. Scientific Report No. 2, Contract No. AF19(604)-5488, University of Colorado, 29 pp.
- Jaeger, J.C., 1953: Conduction of heat in a solid with periodic boundary conditions, with an application to the surface temperature of the Moon. Proc. Cambridge Phil. Soc., 49, 355.

- Junge, C., 1962: Global ozone budget and exchange between stratosphere and troposphere. Tellus, 14, 363-377.
- , 1963: Studies of global exchange processes in the atmosphere by natural and artificial tracers. J. of Geophys. Res., 68, 3849-3855.
- Kaplan, L.D., G. Munch, and H. Spinrad, 1964: An analysis of the spectrum of Mars. Astrophys. J., 139, 1-15.
- Lettau, H., 1951: Theory of surface-temperature and heat transfer oscillation near a level ground surface. Trans. Amer. Geophys. Union, 32, 189.
- Milankovitch, M., 1920: Theorie mathematique des phenomenes thermiques produits par la radiation solaire. Paris sec. 65, 'Le climat de la planete Mars.
- Obasi, G.O.P., 1963: Atmospheric momentum and energy calculations for the southern hemisphere during the IGY. Scientific Report 6, AF19(604)-6108, MIT, 354 pp.
- Ohring, G., 1963: A theoretical estimate of the average vertical temperature distribution in the Martian atmosphere. Icarus, 1, 328-333.
- , and J. Mariano, 1965: Study of the average vertical distribution of temperature in the Martian atmosphere. Final Report Contract No. NAS 9-3423. GCA Corp.
- Prabhakara, C., and J.S. Hogan, 1965: Ozone and carbon dioxide heating in the Martian atmosphere. J. Atmos. Sci., 22, 2, 97-109.
- Sagan, L., and W. Kellogg, 1963: The terrestrial planets. Annual Review of Astronomy and Astrophysics, 1, 235-266.
- Sinton, W.M. and J. Strong, 1960: Radiometric observations of Mars. Astrophys. J., 131, 459-469.
- Spinrad, H., 1962: A search for water vapor and trace constituents in the Venus atmosphere. Icarus, 1, 266-270.
- Wu, S., 1965: A study of heat transfer coefficients in the lowest 400 meters of the atmosphere. J. Geophys. Res., 70, 1801.